# Multiscale energy based suitable wavelet selection for detection of myocardial infarction in ECG

*Sushree Satvatee Swain, Dipti Patra* ✉

*IPCV Lab, Department of Electrical Engineering, National Institute of Technology, Rourkela, India*
✉ *E-mail: dpatra@nitrkl.ac.in*

Published in Healthcare Technology Letters; Received on 8th May 2018; Revised on 31st July 2018; Accepted on 13th August 2018

Over the decades, electrocardiogram (ECG) has been proved as the chief diagnostic tool for assessment of the cardiovascular condition of human being. Myocardial Infarction (MI) is commonly known as heart attack, happens when blood supply stops to heart muscles causing occlusions in some portion or whole artery. MI is the result of three pathological changes such as elevation of ST-segment, the appearance of wide pathological Q-wave and inversion of T-wave in ECG record. Detection of MI by considering few ECG leads generally requires prior information about the pathological behaviour of the disease. The present work considers 12 leads to view the cardiac condition from various angles in ECG signal for accurate detection of MI. This Letter investigates on various wavelet basis functions, i.e. Haar, Daubechies, Symlet, Coiflet and biorthogonal basis filters of different order for selecting the most suitable one for the detection of MI. Wavelet transform of 12-lead ECG signal decomposes the signal into different subbands. A comparative study has been done based on the multiscale energy at different wavelet subbands for the selection of most suitable wavelet basis for the accurate detection of MI. The experimentation is carried out on different datasets from the PTB diagnostic ECG database.

**1. Introduction:** Medical applications would always be in its infancy if engineering applications such as signal processing would not be there. It is quite a difficult task for a healthcare provider to diagnose the abnormality in the heart by seeing the very long electrocardiogram (ECG) records manually at a time. Expertisation in the correct interpretation of the ECG record is a substantive skill for healthcare professionals. So over the years, systematic development has been taken place to lessen the strenuous task of the physicians through automated detection and classification techniques. The graphical representation of the electrical activity of the heart over a period of time is termed as electrocardiogram (ECG). ECG record reflects the periodic depolarisation and repolarisation of atria and ventricles over time. ECG signal is an important tool for the diagnosis of the cardiac condition of a human being [1].

Myocardial Infarction (MI) occurs when blood supply stops to a certain part of the artery or the whole artery. MI is the main cause of death among all cardio vascular diseases worldwide. The myocardium becomes dead without getting the required blood supply, oxygen supply, and essential nutrients [1]. This leads to the deposition of blood platelets, red blood cells, and fibrin and thus forming a local blood clot otherwise known as thrombus [2, 3]. Sometimes thrombolytic substances are detached from the main artery, are driven to some distal arterial tree, and are deposited there. This is followed by blocking of the artery which is termed as the formation of the coronary embolus. This is followed by interruption of blood flow to the artery called as myocardial necrosis. Complete necrosis of the myocardium at risk takes about 4–5 h to happen. Myocardial injury is detected when the level of sensitive and specific biomarkers such as creatine kinase-muscle/brain (CKMB) and cardiac troponin T increases in the blood [4, 5].

The analysis of ECG signal from morphological and pathological background adopts several signal processing methodologies over the past few decades. Analysis of the ECG signal with the help of Fourier transform (FT) spreads the signal in frequency domain but time resolution spread is not achieved [6]. When short time FT (STFT) was applied in signal processing, it provided temporal resolution indicating the changes in the frequency spread with time resolution [7]. The concept of principal component analysis (PCA) and the relationship between PCA and Karhunen–Loeve transform were illustrated and implemented to ECG signal analysis in [8]. PCA techniques have been adopted for ST segment analysis for the detection of myocardial ischemia and other abnormalities related to ventricular repolarisation, atrial fibrillation, and analysis of body surface with potential mapping. Difference between quantitative analysis parameters of vector cardiogram trajectories between the healthy control (HC) and MI cases was found to be significant in [9].

Wavelet transform (WT) method emerged as an effective tool for the analysis of signals with both temporal and frequency resolution levels [6]. Discrete WT (DWT) analysis is the correlation of the signal with the scaled and translated versions of the mother wavelet. The multi-resolution properties of the WT were used for the identification of the fiducial points in the ECG signal [10].

Various methods have been proposed for the detection of MI in earlier literatures. Time sampling methods for extracting ECG morphology features have been adopted for heartbeat fiducial point detection in [11]. Rule-based rough-set decision system has been implemented for the development of a disease inference engine for ECG classification from different standard time plane features in [12]. Time domain features such as Q-wave amplitude, T-wave amplitude, and ST segment deviation are used for automatic detection and localisation of MI using K-nearest neighbour (KNN) [13]. As time domain methods cannot remove artifacts from the frequency bandwidth of the ECG signal, the extracted features are not robust enough to produce remarkable detection accuracy for MI. Thus transform-based methods have been introduced for detection of MI in ECG signal. The entropy in the wavelet domain is used for detection of MI in [9]. A WT-based method has been adopted for ischemia detection in [14]. Neural network approach has been adopted for detection and localisation of MI in [15]. An automated ECG classification system based on a combination of fuzzy logic and neural network theory is presented in [16]. ST-segment analysis approach for ECG interpretation has been implemented in [17]. Some of these techniques use modelling-based schemes by means of training and testing the system. Generally, these modelling-based techniques use only a few ECG leads for analysis of MI that is done on some portion of ECG signal such as ST-segment, ST–T complex instead of the entire ECG segment. This needs the accurate and exact detection of

ST-segment. These processes require prior information about the presence of MI in some of the selected leads. As various kinds of MI is depicted in different leads, monitoring all the 12 leads in multiscale is necessary for better detection of MI. Multiscale principle combined with PCA is adopted to extract deterministic features in statistical process monitoring in [18]. Multiscale PCA approach is proposed for compression of ECG signal in [19].

In this work, an attempt has been made to detect the MI in ECG in terms of its multiscale energy characteristics at different levels of DWT. The analysis is carried out by taking different wavelet basis functions and suitable wavelet basis function for accurate detection of MI.

**2. Wavelet transform:** The WT is a complex link between mathematical facets of functional analysis on one side and theories of subband coding and perfect reconstruction filter banks on the other side. In real time in place of discrete functions, we deal with discrete data. FT is performed to represent a signal as a summation of sinusoids and it is the signal representation in the frequency domain. So this representation is not economical as there is no localisation in time. However, the WT is the representation of the signal in both the time and frequency domains [9]. To detect the onset of MI in ECG recording both time and frequency domain analysis is needed. Thus WT is adopted to trace the point at which the abrupt changes have occurred in the frequency domain at a particular instant of time. The wavelets are compactly supported small waves confined between a finite period of time.

Computation of the wavelet coefficients at every possible scale generates a lot of data. Selection of subsets containing scales and positions as the power of two gives the efficient and accurate result. Thus a DWT generally uses a dyadic grid $a = 2^m$, $m \in Z$ and $b = nb_0 2^m$, $n \in Z$. Assuming $b_0 = 1$ the wavelet function can be defined as

$$\Psi_{m,n}(t) = 2^{-m/2}\Psi(2^{-m}t - n). \tag{1}$$

Corresponding scaling function can be defined as

$$\Phi_{m,n}(t) = 2^{-m/2}\Phi(2^{-m}t - n). \tag{2}$$

The signal is the summation of the signal approximation and the detail coefficient,

$$x(t) = x_M(t) + \sum_{m=-\infty}^{M} d_m(t), \tag{3}$$

where $M$: Decomposition level.

Signal approximation at level $M$ is expressed as

$$x_M(t) = \sum_{n=-\infty}^{n=\infty} S_{M,n}\Phi_{M,n}(t). \tag{4}$$

Detail coefficient of the signal at scale $m$ is expressed as

$$d_m(t) = \sum_{n=-\infty}^{\infty} W_{m,n}\Psi_{m,n}(t), \tag{5}$$

where $S_{M,n} = \langle x(t)\Phi_{M,n}(t)\rangle$: approximation coefficients, $W_{m,n} = \langle x(t)\Psi_{m,n}(t)\rangle$: detail coefficients.

**3. Multiscale energy analysis based optimal wavelet selection for MI detection:** Selection of the suitable mother wavelet filter is very much crucial for any type of processing of ECG signal in the wavelet domain. Suitable basis mother wavelet gives the optimal result in the maximisation of the wavelet coefficients in the wavelet domain. Consequently, it leads to the production of the highest local maxima of the ECG signal. The probability of best frequency characterisation increases upon selection of suitable wavelet filter banks.

In this Letter, multiscale energy analysis of the ECG signal has been performed for detection of MI [20]. Different wavelet basis filters of different orders, i.e. Haar, Daubechies, Symlet, Coiflet, and Biorthogonal basis filters have been used for experimentation for detection of MI. The characteristics of these basis filters are illustrated in Table 1. Different features of ECG signal are confined to different decomposition level of the signal. Incorporating these features multiscale energy analysis is performed with different wavelet basis filters and hence optimal wavelet basis filter is then selected for accurate detection of MI in ECG signal.

Wavelet analysis of an ECG signal with $M$-level decomposition using suitable mother wavelet produces $n^{\text{th}}$ wavelet coefficient at the $M^{\text{th}}$ level [9]. This wavelet analysis is based upon the multiresolution pyramidal decomposition technique and it decomposes the signal up to $M + 1$ subbands. For the $k^{\text{th}}$ ECG lead the decomposition results with an approximation subband coefficients, $cA^k_{M,n}$ at level $M$, and with detail subbands, $cD^k_{m,n}$ at level $m$, where $m = 1, 2, ..., M$. The approximation coefficient is obtained by taking the inner product of the input multilead ECG signal with the scaling function. The detail coefficient is obtained by taking the inner product of the input ECG signal with the wavelet function. In this work, a six-level wavelet decomposition of a 12-lead ECG signal is adopted. The diagnostic and pathological information is distributed over different wavelet subbands basing upon their bandwidth and frequency distribution. The lower frequency subbands contain the most significant information of the ECG signal whereas the higher frequency subbands contain the least significant information.

**Table 1** Popular wavelet families in investigation

| Wavelet family | Haar | Daubechies | Symlets | Coiflets | Biorthogonal |
|---|---|---|---|---|---|
| short term | Haar | Db | Sym | Coif | Bior |
| order $k$ | 1 | $k = 1, 2, ..., 10$ | $k = 2, 3, ..., 8$ | $k = 1, 2, ..., 5$ | $O_R = 1, 2, ..., 6$<br>$O_D = 1, 2, ..., 8$ |
| real/complex | real | real | real | real | real |
| orthogonal/biorthogonal | orthogonal | orthogonal | orthogonal | orthogonal | biorthogonal |
| symmetry | symmetric | asymmetric | nearly-symmetric | nearly-symmetric | asymmetric |
| support width | $k$ | $2k-1$ | $2k-1$ | $6k-1$ | — |
| compactly supported | yes | yes | yes | yes | yes |
| filter length | $2k$ | $2k$ | $2k$ | $6k$ | * |
| number of vanishing moments for $\psi(\theta)$ | $k$ | $k$ | $k$ | $2k$ | — |




doi: 10.1049/htl.2018.5007

3.1. **Multiscale energy analysis**: Wavelet decomposition of 12 lead ECG with M-decomposition level produces $M+1$ subband matrices. The columns of the subband matrix represent the corresponding leads of ECG and the rows represent the coefficients of the subband. Considering $S_{M,n} = A_{M,n}$ and $W_{m,n} = D_{m,n}$, the approximation subband matrix is given by

$$\boldsymbol{A}_M = [cA^1_{M,n}, cA^2_{M,n}, ..., cA^k_{M,n}] \tag{6}$$

and the detail subband matrix is given by

$$\boldsymbol{D}_m = [cD^1_{m,n}, cD^2_{m,n}, ..., cD^k_{m,n}] \tag{7}$$

where $k=12$ is the number of ECG leads and $m = 1, 2, ..., M$. The multiscale matrices contain diagnostic components of the multilead ECG signal. The energy content in the subbands due to wavelet coefficients along each lead is termed as multiscale energy,

$$E^d_m = \frac{1}{N_m}\sum_n |D_{M,n}|^2, \tag{8}$$

$$E^a_m = \frac{1}{N_m}\sum_n |A_{M,n}|^2. \tag{9}$$

It is observed that for all the leads of ECG higher order wavelet subbands (*cA*6; *cD*6; *cD*5; *cD*4) contain large amount of energies and the lower subbands (*cD*3; *cD*2; *cD*1) contain less amount of energies. For the multiscale matrix, the relative energy content of the individual matrix is termed as multiscale multivariate energy contribution efficiency (MMECE)

$$\begin{aligned}\mathrm{MMECE}_{A_L} &= \frac{\mathrm{tr}[C_{A_L}]}{\mathrm{tr}[C_{A_L}] + \sum_{j=1}^{L}\mathrm{tr}[C_{D_j}]} \\ &= \frac{E_{A_L}}{E_{A_L} + \sum_{j=1}^{L} E_{D_j}},\end{aligned} \tag{10}$$

$$\begin{aligned}\mathrm{MMECE}_{D_j} &= \frac{\mathrm{tr}[C_{D_j}]}{\mathrm{tr}[C_{A_L}] + \sum_{j=1}^{L}\mathrm{tr}[C_{D_j}]} \\ &= \frac{E_{D_j}}{E_{A_L} + \sum_{j=1}^{L} E_{D_j}},\end{aligned} \tag{11}$$

where $C_{A_L}, E_{A_L}$ and $C_{D_j}, E_{D_j}$ represent the covariance matrices and energies in approximation and detail matrices, respectively. Fig. 1 describes the block diagram for the proposed multiscale energy analysis based optimal wavelet selection.

**4. Results and discussions:** Here the MI data are taken from the PTB diagnostic ECG database [21]. This database includes digitised ECG data recorded from HC cases and different cardiac disease cases at the Department of Cardiology, University Clinic Benjamin Franklin in Berlin, Germany. The database contains 549 records from 290 subjects. The different subjects include MI: 148, cardiomyopathy/heart failure: 18, bundle branch block: 15, dysrhythmia: 14, myocardial hypertrophy: 7,valvular heart disease: 6, myocarditis: 4, miscellaneous: 4 and healthy controls: 52. In this investigation, 12 lead ECG records are considered simultaneously for proper viewing of heart from every possible angle. All the Matlab simulated experimental results are presented using ECG *S*0017*lrem* recording of PTB diagnostic ECG database. The 12 lead ECG data are first fed to the preprocessing block. The preprocessing block constitutes a filtering method which adopts a moving average filter to remove the base line wanders, muscle artifacts, baseline drifts and powerline interfaces from the multilead ECG recordings. For high frequency removal, we introduced a discrete cosine transform (DCT)-based bandpass filter whose pass band is set to a frequency interval $[f_1 f_2]$ so as to eliminate the influence of remaining low frequency artifacts and high frequency noise including the electromyography noise. $f_1$ is chosen so that it does not exceed the cardiac fundamental frequency (CFF), whereas $f_2$ is considered as 45 Hz, which is slightly lower than the powerline frequency. First, QRS complexes are extracted using a bandpass filter. Its passband is set at [5 Hz, 15 Hz]. Then the QRS complexes are transformed using DCT, in which the first dominant frequency is considered as CFF.

Then the frame based segmentation is carried out to acquire the correlation information between the leads, between the rhythms and between the samples. After preprocessing the multilead ECG signal is subjected to WT for decomposition. The choice of six level decomposition $L$, which satisfy the frequency range of the main features of an ECG is based on sampling frequency $F_s$ and is given as $L = [\log_2(F_s - 2.96)]$ [22]. Here $L$ is an integer number, and $F_s$ is the sampling frequency of the signal. Here different wavelet basis filters have been adopted and thus suitable basis filter is selected for the detection of MI.

Fig. 2 presents the 12 lead ECG *S*0017*lrem* recording taken from the PTB diagnostic ECG database.

Fig. 3 presents the lead I ECG recording of the given MI data, i.e. ECG *S*0017*lrem* recording taken from the PTB diagnostic ECG database. All the 12 lead ECG signals are subjected through wavelet decomposition with different wavelet basis filters under investigation, i.e. Haar, Daubechies, Symlet, Coiflet and biorthogonal basis filters of different orders. The six level wavelet decomposition of the same ECG recording using Haar wavelet basis function is shown in Fig. 4. The sixth level approximation subband a6 for the same ECG recording with several wavelet basis filters is shown in Fig. 5. Then the MMECE of the subband matrices is calculated for different subbands.

The MMECE plot of the MI ECG record decomposed with Daubechies biorthogonal 9/7 filter is shown in Fig. 6. The relative energy distribution, i.e. energy percentage of all the individual matrices is calculated. It is observed that the matrices A6, D6,

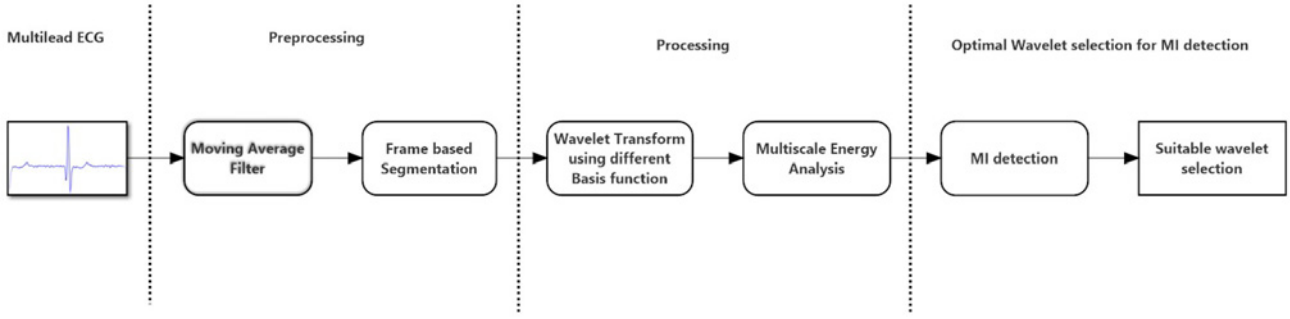


**Fig. 1** *Block diagram of proposed work*

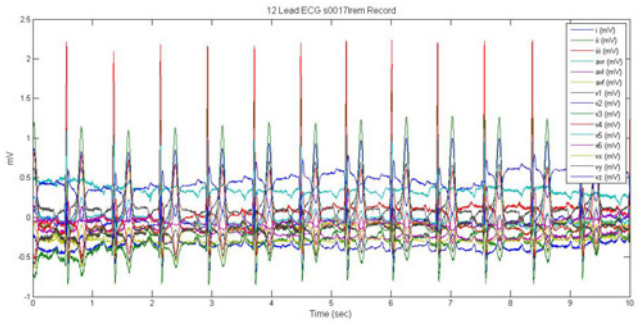


**Fig. 2** *12 lead MI ECG data*

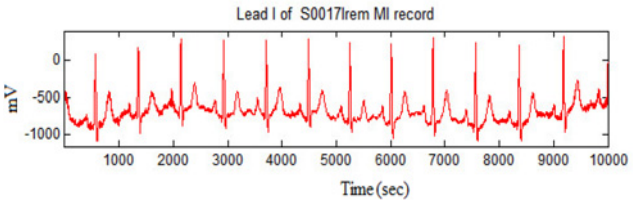


**Fig. 3** *Lead I of tested MI ECG data*

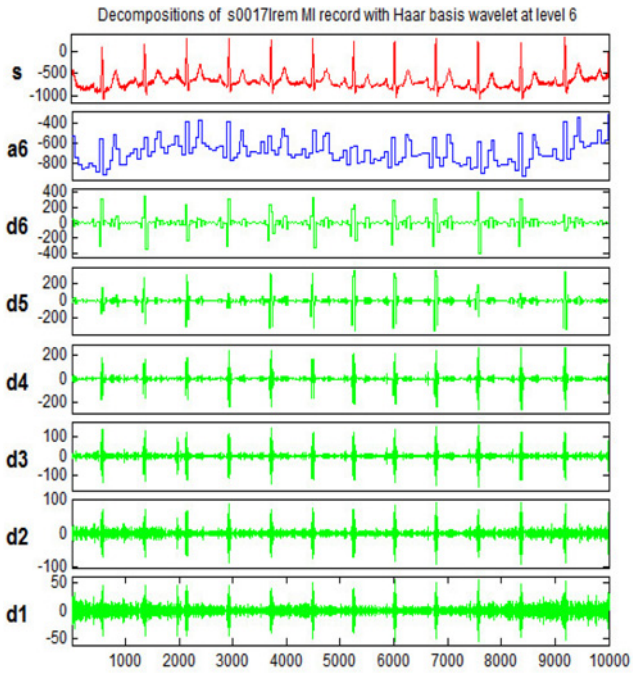


**Fig. 4** *Six level decomposition of ECG (MI) with Haar basis filter*

D5 and D4 (higher order subbands) contain more amount of energy whereas matrices D3, D2 and D1 (lower order subbands) contain less amount of energy, which is illustrated in Table 2 for the above-mentioned ECG signal with MI. The reason for choosing higher-order subbands is that the higher order subbands contain vital clinical diagnostic information of more energy. Lower order subbands contain relatively less energy due to the availability of less clinical information.

The difference of ECG energy distribution between MI subjects and healthy controls (HC) is shown in Table 3. As observed from this table, there is the difference between energy distribution for HC and MI classes for lead I, lead II and lead aVL. These

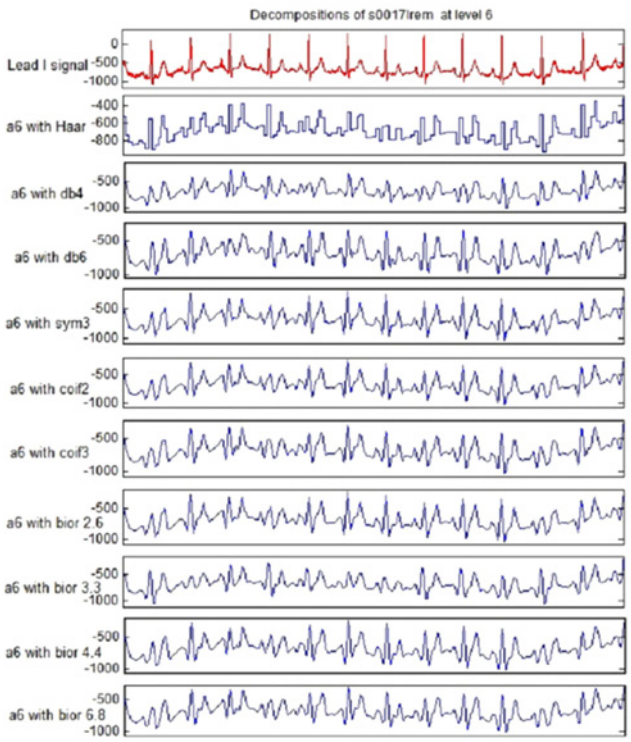


**Fig. 5** *Six level decomposition of ECG (MI) with different basis wavelets*

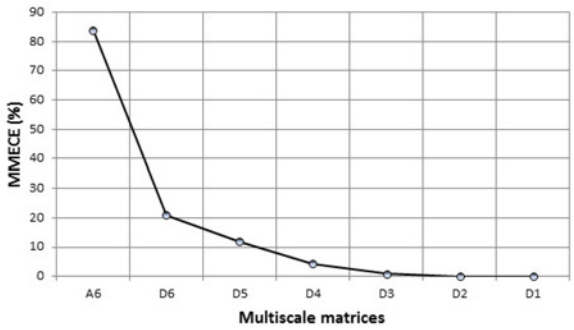


**Fig. 6** *Energy contribution of multiscale multivariate matrices in terms of MMECE for 12 lead ECG MI data from PTB diagnostic ECG database*

**Table 2** Energy percentage distribution of subbands

| Lead | A6 (%) | D6 (%) | D5 (%) | D4 (%) | D3 (%) | D2 (%) |
|---|---|---|---|---|---|---|
| I | 97.52 | 1.55 | 0.81 | 0.10 | 0.01 | 0.01 |
| II | 98.84 | 0.59 | 0.40 | 0.13 | 0.02 | 0.02 |
| III | 93.41 | 5.20 | 1.00 | 0.20 | 0.11 | 0.08 |
| aVR | 98.54 | 0.77 | 0.56 | 0.11 | 0.01 | 0.01 |
| aVL | 94.76 | 3.81 | 1.25 | 0.11 | 0.04 | 0.03 |
| aVF | 98.07 | 1.32 | 0.35 | 0.16 | 0.05 | 0.04 |
| V1 | 94.74 | 4.54 | 0.56 | 0.11 | 0.03 | 0.01 |
| V2 | 90.18 | 7.42 | 2.10 | 0.27 | 0.02 | 0.01 |
| V3 | 82.00 | 11.33 | 5.75 | 0.90 | 0.02 | 0.01 |
| V4 | 92.05 | 4.81 | 2.76 | 0.36 | 0.01 | 0.01 |
| V5 | 7.49 | 15.64 | 9.26 | 1.43 | 0.11 | 0.07 |
| V6 | 96.99 | 2.00 | 0.89 | 0.10 | 0.01 | 0.01 |

differences in energy distribution are due to the pathological alteration in the clinical features during the onset of MI [23].

The within-class variations of normalised multiscale wavelet energy for all ECG leads are evaluated using 1074 MI multilead

**Table 3** Energy distribution between MI subjects and healthy controls

| Subband | HC (%) | MI (%) | HC (%) | MI (%) | HC (%) | MI (%) |
|---|---|---|---|---|---|---|
| A6 | 91.65 | 65.08 | 96.81 | 99.14 | 93.67 | 70.40 |
| D6 | 3.68 | 24.73 | 1.90 | 0.56 | 4.11 | 26.51 |
| D5 | 3.17 | 6.96 | 1.22 | 0.23 | 1.93 | 2.04 |
| D4 | 0.32 | 1.27 | 0.07 | 0.06 | 0.25 | 0.51 |
| D3 | 0.34 | 0.97 | 0.01 | 0.01 | 0.03 | 0.32 |
| D2 | 0.39 | 0.74 | 0.00 | 0.00 | 0.00 | 0.17 |
| D1 | 0.44 | 0.24 | 0.00 | 0.00 | 0.00 | 0.05 |

ECG frames. The normalised multiscale energy of subband A6 is shown in Fig. 7. The normalised multiscale energy of subbands D6, D5 and D4 are presented here as these subbands carry the most vital information. The normalised multiscale energy of subbands D6, D5 and D4 are shown in Figs. 8–10, respectively. The normalised multiscale energy of these four subbands is different and this is due to the difference in the pathological information of ECG signal in higher order subbands.

After multiscale wavelet energy analysis the multiscale features such as mean, standard deviation, median, median absolute deviation and mean absolute deviation are computed for individual leads. It is observed that the mean, standard deviation, median, median absolute deviation and mean absolute deviation are different for different scales. The above parameters for the considered ECG with MI are analysed and given in Table 4.

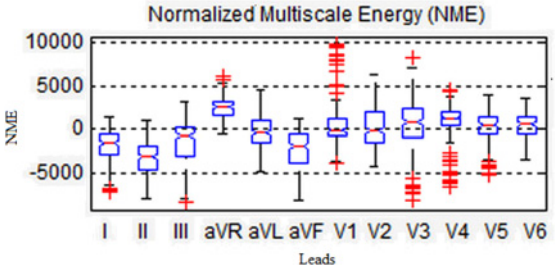


**Fig. 7** *Variation of multiscale energy for cA6 subbands for 12 ECG leads in MI record*

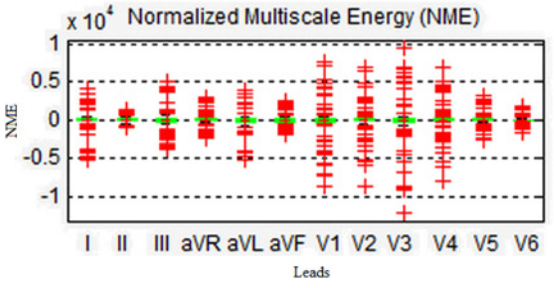


**Fig. 8** *Variation of multiscale energy for cD6 subbands for 12 ECG leads in MI record*

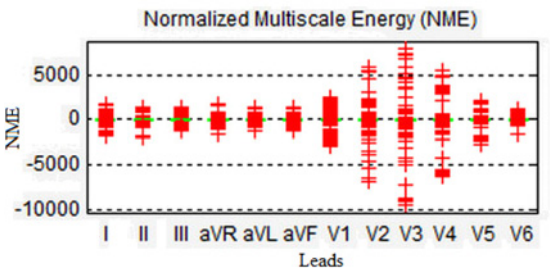


**Fig. 9** *Variation of multiscale energy for cD5 subbands for 12 ECG leads in MI record*

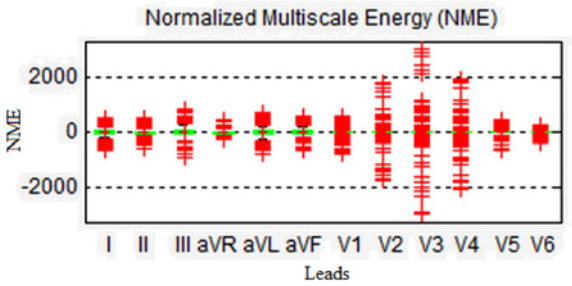


**Fig. 10** *Variation of multiscale energy for cD4 subbands for 12 ECG leads in MI record*

From this table, it is observed that there is very large difference between the mean and standard deviation among all the 12 leads of the ECG signal, as all the leads view the heart at a different angle. The mean values of leads I, II, III, aVL, aVF, V5, and V6 are very low and it specifies that these leads undergo the infarction in arteries. Inferior MI is depicted from the leads II, III, and aVF whereas left lateral MI is traced out from leads I, V5, V6, and aVL. Thus the analysis says that the infarction is an inferolateral infarction. The standard deviations of corresponding leads are high which confirms the abrupt changes of normal ECG shape. Further analysis is performed considering different MI data and for the same MI data different wavelet basis filters are used for selection of suitable wavelet basis filter. In our investigation, we have examined 110 MI records for detection of infarcted ECG records. All the records are taken from the PTB diagnostic ECG database. Detection accuracy is computed considering two factors, i.e. MI record analysed and MI record detected into account.

$$\text{Detection accuracy} = \frac{\text{MI records detected}}{\text{MI records analysed}} \times 100. \quad (12)$$

Detection accuracy is computed considering the wavelet basis functions under test. A complete comparative study of detection accuracy using different wavelet basis functions such as Haar, Daubechies, Symlet, Coiflet, and Biorthogonal basis filters is presented in Fig. 11. From the comparison, it is found that detection accuracy is maximised for Daubechies 9/7 biorthogonal wavelet filter followed by Daubechies 6/8 biorthogonal wavelet basis

**Table 4** Feature analysis of different leads

| Lead | Mean | Standard deviation | Median | Median absolute deviation | Mean absolute deviation |
|---|---|---|---|---|---|
| I | −683.372 | 173.764 | 714 | 82 | 117.817 |
| II | −659.696 | 249.725 | −624 | 134 | 189.471 |
| III | −24.850 | 292.671 | 88 | 158 | 223.420 |
| aVR | 672.046 | 157.564 | 681 | 68 | 102.731 |
| aVL | −353.517 | 205.900 | −386 | 104 | 151.416 |
| aVF | −317.466 | 257.879 | −255 | 132 | 200.126 |
| V1 | 296.576 | 386.902 | 210 | 94 | 262.851 |
| V2 | 132.112 | 605.299 | −60 | 129 | 429.275 |
| V3 | 100.977 | 874.756 | −232 | 141 | 640.183 |
| V4 | 24.871 | 755.270 | −234 | 89 | 473.206 |
| V5 | 1.555 | 309.679 | −59 | 76 | 154.420 |
| V6 | −86.759 | 148.650 | −106 | 60 | 89.213 |

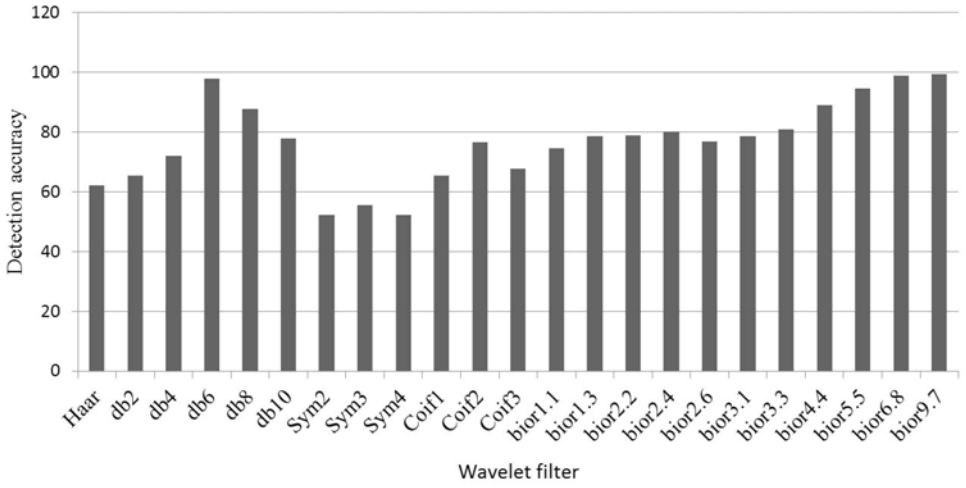


**Fig. 11** *Comparative result of detection accuracy of MI with wavelet basis functions under test*

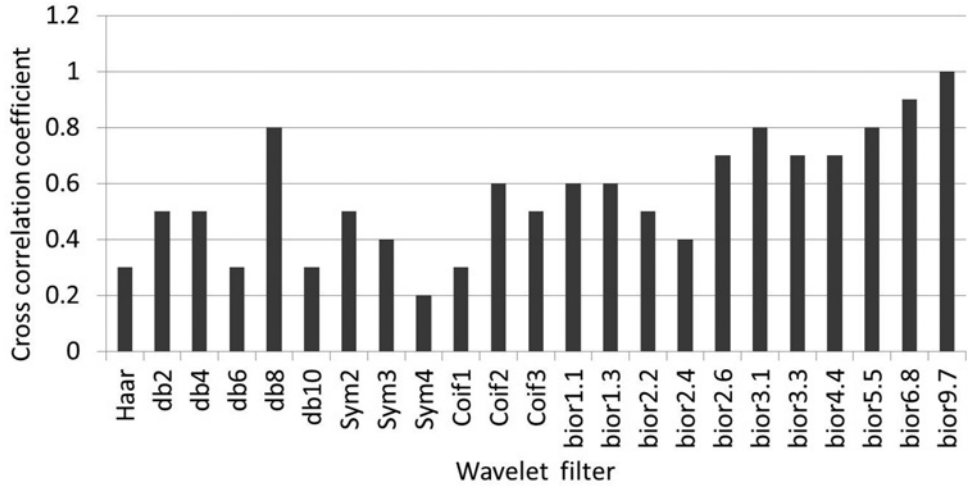


**Fig. 12** *Comparative result of correlation coefficients with wavelet basis functions under test*

filter. The comparative study conveys that the more is the similarity between the selected basis function and the ECG data, higher is the detection accuracy. Fig. 12 represents similarity measure cross-correlation coefficients of the ECG signal with different wavelet basis filters of a different order. The result of cross correlation coefficients strengthens the suitability of Daubechies 9/7 biorthogonal wavelet filter for the detection of MI since this filter produces a maximum cross correlation coefficient.

In the investigation, we performed experiments following the multiscale energy analysis method for obtaining suitable basis filter to detect MI in the ECG signal. From the experimental results, it is observed that the Daubechies 9/7 biorthogonal wavelet filter is most appropriate for the detection of MI in the ECG signal.

**5. Conclusion:** In this Letter, a multiscale energy analysis approach has been adopted for the detection of MI. This work also aims at selection of suitable wavelet basis function for detection of MI. Most of the ongoing and present works concentrate on only fewer leads of the ECG signal. Thus it is quite difficult to exactly detect the presence of MI from the ECG recordings. The proposed MI detection technique does not require any prior knowledge of the pathological characteristics of the MI. Here multiscale multilead energy features are taken into consideration for detection of MI. Since all the leads are analysed at one time the simultaneous changes that occur in the leads are properly traced out here. Thus the analysis provides the detection of MI with the accurate investigation of all the ECG leads. This proposed technique helps in immediate detection of MI with accuracy, which can be interpreted within 10 min of onset of MI. Thus it is very advantageous than the biochemical marker test which takes almost 6–9 h. The experimental results specify the suitability of Daubechies 9/7 biorthogonal wavelet basis function to be the most suitable and appropriate wavelet basis function for the detection of MI in the ECG signal. The selected wavelet basis function is found to be optimal in terms of detection accuracy and experimentation on cross correlation coefficients further strengthens the suitability of the selected basis function.

**6. Funding and declaration of interests:** Conflict of interest: None declared.

## 7 References

[1] Hall J.E.: 'Text book of medical physiology' (Elsevier Health Sciences, New York, NY, USA, 2006, 11th edn.)
[2] Goldberger A.L.: 'Clinical electrocardiography: a simplified approach' (Elsevier Health Sciences, New York, NY, USA, 2012)

[3] Morrow D.A.: 'Myocardial infarction: a companion to Braunwald's heart disease' (Elsevier Health Sciences, New York, NY, USA, 2016)
[4] Goodman S.G., Steg P.G., Eagle K.A., *ET AL.*: 'The diagnostic and prognostic impact of the redefinition of acute myocardial infarction: lessons from the global registry of acute coronary events (grace)', *Am. Heart J.*, 2006, **151**, (3), pp. 654–660
[5] Thygesen K., Alpert J.S., Jaffe A.S., *ET AL.*: 'Third universal definition of myocardial infarction', *Eur. Heart J.*, 2012, **33**, (20), pp. 2551–2567
[6] Addison P.S.: 'Wavelet transforms and the ECG: a review', *Physiol. Meas.*, 2005, **26**, (5), p. R155
[7] Gramatikov B., Georgiev I.: 'Wavelets as alternative to short-time Fourier transform in signal-averaged electrocardiography', *Med. Biol. Eng. Comput.*, 1995, **33**, (3), pp. 482–487
[8] Castells F., Laguna P., Sörnmo L., *ET AL.*: 'Principal component analysis in ECG signal processing', *EURASIP J. Adv. Signal Process.*, 2007, **2007**, (1), p. 074580
[9] Jayachandran E.S., Joseph K.P., Acharya U.R., *ET AL.*: 'Analysis of myocardial infarction using discrete wavelet transform', *J. Med. Syst.*, 2010, **34**, (6), pp. 985–992
[10] Ranjith P., Baby P., Joseph P.: 'ECG analysis using wavelet transform: application to myocardial ischemia detection', *ITBM-RBM*, 2003, **24**, (1), pp. 44–47
[11] De-Chazal P., O'Dwyer M., Reilly R.B.: 'Automatic classification of heartbeats using ECG morphology and heartbeat interval features', *IEEE Trans. Biomed. Eng.*, 2004, **51**, (7), pp. 1196–1206
[12] Mitra S., Mitra M., Chaudhuri B.B.: 'A rough-set-based inference engine for ECG classification', *IEEE Trans. Instrum. Meas.*, 2006, **55**, (6), pp. 2198–2206
[13] Arif M., Malagore I.A., Afsar F.A.: 'Detection and localization of myocardial infarction using k-nearest neighbor classifier', *J. Med. Syst.*, 2012, **36**, (1), pp. 279–289
[14] Papaloukas C., Fotiadis D.I., Likas A., *ET AL.*: 'Automated methods for ischemia detection in long duration ECGs', *Cardiovasc. Rev. Rep.*, 2003, **24**, (6), pp. 313–319
[15] Hedén B., Öhlin H., Rittner R., *ET AL.*: 'Acute myocardial infarction detected in the 12-lead ECG by artificial neural networks', *Circulation*, 1997, **96**, (6), pp. 1798–1802
[16] Lu H., Ong K., Chia P.: 'An automated ECG classification system based on a neuro-fuzzy system'. Computers in Cardiology 2000, 2000, pp. 387–390
[17] Sun L., Lu Y., Yang K., *ET AL.*: 'ECG analysis using multiple instance learning for myocardial infarction detection', *IEEE Trans. Biomed. Eng.*, 2012, **59**, (12), pp. 3348–3356
[18] Bakshi B.R.: 'Multiscale PCA with application to multivariate statistical process monitoring', *AIChE J.*, 1998, **44**, (7), pp. 1596–1610
[19] Sharma L., Dandapat S., Mahanta A.: 'Multichannel ECG data compression based on multiscale principal component analysis', *IEEE Trans. Inf. Technol. Biomed.*, 2012, **16**, (4), pp. 730–736
[20] Swain S.S., Patra D.: 'Analysis of myocardial infarction using wavelet transform and multiscale energy analysis'. TENCON 2017–2017 IEEE Region 10 Conf., 2017, pp. 1640–1645
[21] Oeff M., Koch H., Bousseljot R., *ET AL.*: 'The PTB diagnostic ECG database', National Metrology Institute of Germany, 2012. Available at http://www physionet org/physiobank/database/ptbdb
[22] Al-Fahoum A.S.: 'Quality assessment of ECG compression techniques using a wavelet-based diagnostic measure', *IEEE Trans. Inf. Technol. Biomed.*, 2006, **10**, (1), pp. 182–191
[23] Tripathy R., Dandapat S.: 'Detection of myocardial infarction from vectorcardiogram using relevance vector machine', *Signal. Image Video Process.*, 2017, **11**, (6), pp. 1139–1146